Available online at www.sciencedirect.com
SCIENCE DIRECT®
Surface Science 572 (2004) 1–10
SURFACE SCIENCE
www.elsevier.com/locate/susc

The $(\sqrt{7} \times \sqrt{7})R19.1°$-$C_6H_6$ adsorption structure on Co{0001}: a combined Tensor LEED and DFT study

K. Pussi [a,*], M. Lindroos [a], J. Katainen [b], K. Habermehl-Ćwirzeń [b], J. Lahtinen [b], A.P. Seitsonen [c]

[a] *Institute of Physics, Tampere University of Technology, P.O. Box 692, 33101 Tampere, Finland*
[b] *Laboratory of Physics, Helsinki University of Technology, P.O. Box 1100, 02015 HUT, Finland*
[c] *Physikalisch Chemisches Institut, Universität Zürich, Winterthurerstr. 190, CH-8057 Zürich, Switzerland*

Received 15 June 2004; accepted for publication 10 August 2004
Available online 11 September 2004

Abstract

The geometric structure of a Co{0001}-$(\sqrt{7} \times \sqrt{7})R19.1°$–$C_6H_6$ surface formed by adsorption of benzene to the saturation coverage at 170 K has been determined by low energy electron diffraction (LEED). The favored model consists of a flat laying, nearly undisturbed benzene molecule, with the hydrogen–carbon bonds bent away from the substrate by 0.3 ± 0.2 Å. The carbon ring lies at a hcp-site with the two parallel C–C bonds aligned with $[1\bar{1}00]$ direction. Buckling between the inequivalent carbon atoms in the molecular ring is within the experimental uncertainty (0.01 ± 0.11 Å). The experimental results are supported by density functional calculations.

Keywords: Low energy electron diffraction (LEED); Density functional calculations; Surface structure, morphology, roughness, and topography; Cobalt; Aromatics

1. Introduction

The adsorption of benzene on metallic surfaces is of considerable interest because it serves as a model system for more complicated cyclic hydrocarbons. The bonding of aromatic hydrocarbons plays an important role in many catalytic processes. Determination of the detailed adsorption geometry of the benzene molecule is hence of fundamental importance. The main issues being discussed in the past have been the magnitude of substrate induced distortions on the molecule and the effect of the neighboring molecules on the choice of the adsorption site and orientation.

* Corresponding author. Tel.: +358 3 3115 2681; fax: +358 3 3115 2600.
E-mail address: katarina@ee.tut.fi (K. Pussi).

0039-6028/$ - see front matter
doi:10.1016/j.susc.2004.08.017

Electron spectroscopic techniques seem to agree that the preferred bonding geometry generally involves a flat lying π-bonded aromatic ring [1–3], while the general picture from the crystallographic studies, which have mostly been done on hexagonal close packed surfaces, is of flat π-bonded molecular adsorption with a small increase in the diameter of the carbon ring along with small Kekulé type distortions and possible benzene induced substrate distortions [4–10].

Habermehl-Ćwirzeń et al. have studied benzene on Co{0001} surface by X-ray photoelectron spectroscopy, thermal desorption spectroscopy, low energy electron diffraction and work function measurements [1]. They found that benzene adsorbs molecularly at room temperature and forms a $c(2\sqrt{3}\times 4)rect$ surface structure with $\Theta = 0.125$ ML. At lower temperatures slightly higher coverages ($\Theta = 0.14$ ML) were observed and the structure changed to a $p(\sqrt{7}\times\sqrt{7})R19^\circ$. They also reported that during heating above 340 K benzene partially dehydrogenates as evidenced by desorption of hydrogen. Rest of the molecule stays at the surface and formation of a possible hydrocarbon molecule C_6H_5 was suggested. The desorption of molecular benzene was negligible.

Barnes et al. have reported an ARUPS study of a benzene saturated Co{10$\bar{1}$0} surface at 300 K where an ordered $p(3\times 1)$ monolayer is formed [11]. In contrast to the earlier studies the photoemission data indicates a molecule, which is strongly tilted and/or distorted. This unusual result has been confirmed by Pussi et al. in a Tensor LEED study of the same adsorption phase [12] where they found that benzene adsorption occurs with the molecular ring in a tilted geometry across the substrate close packed [12$\bar{1}$0] atomic rows in an off-center bridge site with C_S symmetry.

A number of face-capping complexes with similar adsorption environment than cobalt basal plane exist with benzene ligands bound to cobalt clusters. In these cluster compounds only slight distortion of the Kekulé type has been observed (< 0.01 Å). The carbon ring remains rather similar compared to the gas phase with the carbon–carbon bonds alternating between 1.405 Å and 1.449 Å. The cobalt–carbon bond lengths remain also similar to the sum of cobalt metallic radii and carbon single bond covalent radii (2.04 Å), ranging between 2.011 Å and 2.069 Å [13].

One aspect of this study is to find out whether the unusual adsorption geometry of benzene on cobalt {10$\bar{1}$0} surface found in earlier studies by Barnes et al. [11] and Pussi et al. [12] is due the open surface structure or due to the fact that the substrate is cobalt. On the other hand the effect of cobalt on the bonding of the carbons in the benzene molecular ring is of interest. It is possible that cobalt weakens the carbon–carbon bonds in the molecular ring as has been seen in the two earlier studies of benzene on cobalt [11,12]. This paper continues the study of benzene on Co{0001} surface started by Habermehl-Ćwirzeń et al. [1] and presents the detailed geometry and adsorption site of the Co{0001}-$(\sqrt{7}\times\sqrt{7})R19.1^\circ$–$C_6H_6$ phase studied by Tensor LEED and density functional theory calculations. In the next sections experimental and theoretical procedures are explained as well as results of this study are presented and compared to other similar studies.

2. LEED experiments and analysis

2.1. Experimental

The LEED experiments were performed in a stainless steel UHV chamber with a base pressure of 2×10^{-10} Torr. Beside the LEED system, the apparatus was equipped with facilities for X-ray photoelectron spectroscopy (XPS) and thermal desorption spectroscopy (TDS).

The specimen (Co{0001} single crystal) was attached to the sample holder by spot welded tantalum wires. The Co{0001} sample was cleaned by argon ion sputtering and subsequent annealing. The cleanliness of the cobalt surface was verified by XPS.

After annealing the sample was cooled down to the adsorption temperature of 220 K. As this took about 15 min, a clean surface was not warranted due to residual gas adsorption. To ensure the cleanliness, the sample was then flashed up to 500 K and cooled again. As the sample's surrounding was still at very low temperature, the second cooling took a negligible amount of time.

Benzene, with a nominal purity of 99.5%, was used in this experiment after additional purification. The purification took place by repeated freezing and thawing cycles.

As stated in Ref. [1], two diffraction patterns were found for benzene adsorption on Co{0001} depending on the adsorption temperature and benzene exposure: $c(2\sqrt{3}\times 4)rect$ and $p(\sqrt{7}\times\sqrt{7})R19.1^\circ$. The nominal coverages for these structures are 1/8 and 1/7, indicating that the distance between neighboring molecules is quite small and the actual positions of the molecules on the surface are rather similar. The $p(\sqrt{7}\times\sqrt{7})R19.1^\circ$ structure was chosen to be analyzed in detail, since it corresponds to the saturation coverage at 220 K.

In order to achieve the best possible contrast and sharpness of the diffraction pattern, LEED-*IV* scans were made after dosing 50 L benzene at 220 K. The *IV* data were recorded at 170 K by a CCD camera attached to the system.

During the measurement the acceleration voltage was raised in steps of 2 eV and at each step two pictures from the diffraction pattern were averaged and saved. This resulted in a series of pictures, which served for the off-line analysis of the *IV* curves. Normal incidence was attained by visual investigation of the equivalent beams before each measurement and further ensured during off-line analysis. To reduce unnecessary radiation damage the sample was negatively biased to repel the electron beam during parameter adjustment and grounded only during capturing of the pictures. To further reduce the radiation damage the diffraction patterns were recorded in short 40–100 eV parts, which overlap each other for at least 10 eV. The overlap was used to ensure that the *IV* curve intensity level between subsequent measurements was equal.

The *IV* data consist of 10 beams $((1,0),(1,1),(2,0),(\frac{2}{7},\frac{1}{7}),(\frac{1}{7},\frac{4}{7}),(\frac{4}{7},\frac{2}{7}),(\frac{3}{7},\frac{5}{7}),(\frac{6}{7},\frac{3}{7}),(\frac{2}{7},\frac{8}{7})$ and $(\frac{9}{7},\frac{1}{7})$ collected at normal incidence with energies between 20 and 500 eV. The cumulative energy range is 1470 eV. Since the $(\frac{2}{7},\frac{8}{7})$ and $(\frac{9}{7},\frac{1}{7})$ were experimentally observed to overlap each other over most of their energy range, these two beams were averaged together in the end of the analysis to produce just one beam which is labeled $(\frac{2}{7},\frac{8}{7})$.

2.2. Theoretical considerations

The multilayer relaxation and reconstruction of benzene-covered cobalt surface has been analyzed using Tensor LEED codes of Van Hove et al. [14]. Prior to the theoretical analysis each beam was individually background corrected by fitting an exponentially increasing function to user chosen minima. The exponential increase in the background intensity level is caused by the diffraction spots approaching each other when the energy is increased. Symmetrically equivalent beams were then averaged together in order to increase the signal to noise level and compensate for any remaining deviation of the angular alignment.

Theoretical $I(V)$ spectra were calculated in range for 20–520 eV. Phase shifts up to $l_{max} = 8$ were used to describe the scattering properties of carbon, cobalt and hydrogen which were calculated using Barbieri/Van Hove Phaseshift package [15]. Hydrogen atoms were ignored in the preliminary stage of the analysis, because of their weak scattering properties for low energy electrons [16]. In the further stages of the analysis, the hydrogen atoms were added to the calculation. Other nonstructural parameters include Debye temperatures (Θ_D) for cobalt (385 K), for carbon (420 K) and for hydrogen (5000 K) and an energy independent imaginary part of inner potential ($V_I = -5$ eV). The high Debye temperature value is needed for hydrogen in order to get reasonable small vibration amplitude. The vibrations of atoms were modeled as isotropic in the analysis. The 1-D components of the vibration amplitudes that correspond to the Debye temperatures used are 0.06 Å, 0.12 Å and 0.09 Å for cobalt, carbon and hydrogen respectively. For cobalt, a layer dependent Debye temperature was used i.e. different values of Debye temperature for the surface and the bulk atoms. The real part of the inner potential was assumed to be energy independent and was allowed to shift to obtain an optimal theory–experiment agreement as a standard procedure of LEED analysis.

The experimentally observed LEED pattern possesses high symmetry of sixfold rotation axis (C_6). Because none of the adsorption sites has that symmetry, proper domain averaging has to be

taken into the analysis. Agreement between theory and experiment was tested using Pendry R-factor and error bars quoted are calculated using Pendry RR-function [17].

3. Density functional theory calculational details

The density functional theory (DFT) calculations were performed in the Kohn–Sham formalism, with the generalized gradient approximation (GGA) of Perdew et al. [18] as the exchange-correlation functional. The plane wave basis [19] was employed. The cut-off energy was set to 37 Ry, and the surface was modeled with a slab geometry with five substrate layers and ca. 12 Å of vacuum. The two outer-most substrate layers were relaxed. Simulations were done with one benzene molecule in the primitive $(\sqrt{7}\times\sqrt{7})R19.1^\circ$ unit cell. A 4×4 $\overline{\Gamma}$ point centered Monkhorst–Pack grid was used for the k point sampling, yielding $4k$ points in the irreducible wedge of the Brillouin zone. While calculating the vibrational frequencies via finite differences only Γ point was used. The calculated lattice constants in bulk cobalt $a = 2.477$ Å and $c/a = 1.614$ compare well with the experimental values 2.51 Å and 1.622. The magnetic moment comes out as 1.625 μ_B, again in good agreement with the experiments (1.72 μ_B) [20].

4. Results

In the first stage of the analysis preliminary search for the possible structures was done. There were eight possible high-symmetry adsorption sites to be considered: two top sites (top A and top B), two hcp sites (hcp A and hcp B), two fcc sites (fcc A and fcc B) and two bridge sites (bridge A and bridge B). The two different high symmetry orientations (A and B) of the benzene molecule correspond to A: the two parallel C–C bonds are aligned with $[1\,\bar{1}\,0\,0]$ direction and B: the two parallel C–C bonds are aligned with $[1\,1\,\bar{2}\,0]$ direction. These sites are shown in Fig. 1. On the top, hcp and fcc sites sixfold symmetry (D_{6h}) of the gas phase benzene reduces to threefold symmetry (C_3) and on the bridge sites symmetry reduces to C_1. Therefore sites with the threefold symmetry axis have two domains and the bridge sites have six possible domains.

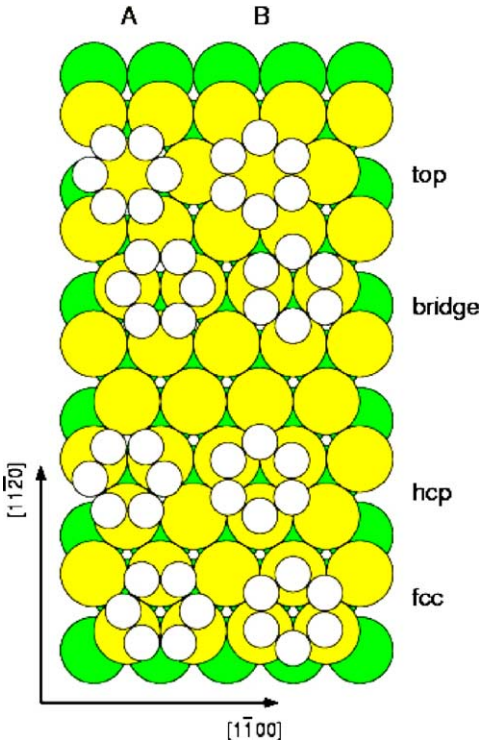

Fig. 1. High-symmetry adsorption sites. Main crystallographic directions are indicated with arrows. Carbon atoms and the two top cobalt layers are shown.

In the preliminary search the only parameter varied was the metal–carbon bond length. A range of bond lengths covered was from 1.8 Å to 2.4 Å in steps of 0.05 Å. This range was considered to cover the reasonable bond length range for the sum of cobalt metallic radii (1.26 Å) and the carbon covalent single bond radii (0.78 Å) of 2.04 Å. The benzene ring was kept flat and the C–C bond length was at 1.39 Å, which is the C–C bond length value for the gas phase benzene. At this stage the non-structural parameters were not optimized, aside for the real part of the inner potential.

Trial geometries were selected for further analysis using Pendry's RR-method [17]. The variance is calculated as a product of the minimum Pendry R-factor and the Pendry RR-function. Structures with the Pendry R-factor outside the sum of the

Table 1
Pendry *R*-factors from different stages the of analysis

Geometry	R_P (stage 1)	R_P (stage 2)	R_P (stage 3)
Top A	0.35	0.33	–
Top B	0.38	0.35	–
fcc A	0.47	–	–
fcc B	0.53	–	–
hcp A	0.36	0.27	0.26
hcp B	0.50	–	–
Bridge A	0.36	0.32	–
Bridge B	0.49	–	–
Variance by Pendry's RR-method [17]	0.06	0.04	0.04

Last line indicates the variance calculated using Pendry's RR-method [17]. Structures with Pendry *R*-factors outside the variance are excluded from further analysis.

variance and the minimum Pendry *R*-factor were discarded from further analysis. The value of the Pendry RR-function of 0.16 led to a variance of 0.06 after the preliminary stage, which meant that there were four sites left for the second stage: top A, top B, hcp A and bridge A. In the second stage of the analysis the hydrogen atoms were added to the calculation and relaxations perpendicular to the surface were allowed for the benzene and for the first four cobalt layers. The results from the first and the second stage are shown in Table 1.

After the second stage there was only one possible geometry left for the third stage of the analysis, hcp A ($R_P = 0.27$), which was again selected using the Pendry's RR-method. In the final refinement stage the imaginary part of the inner potential (−5 eV) and the Debye temperatures for the surface cobalt (280 K, vibration amplitude of 0.08 Å), carbon (420 K) and hydrogen (1600 K, vibration amplitude of 0.16 Å) were optimized. For the cobalt bulk layers (second layer and deeper) the Debye temperature was not optimized. The phase shifts were recalculated for the favored structure. Lateral relaxation of the first layer cobalt, the carbon (stretching of C-ring) and the hydrogen atoms did not lead to significant improvement in the agreement. The final value of the Pendry *R*-factor is 0.26. Fig. 2(a) shows the top view and Fig. 2(b) the side view of the optimum geometry.

Our results imply relatively weak interaction between the substrate cobalt and the carbon in the benzene. The average perpendicular distance between the molecular ring and the first cobalt layer ($dz_{C–Co}$) is 2.20 ± 0.09 Å. The shortest C–Co bond

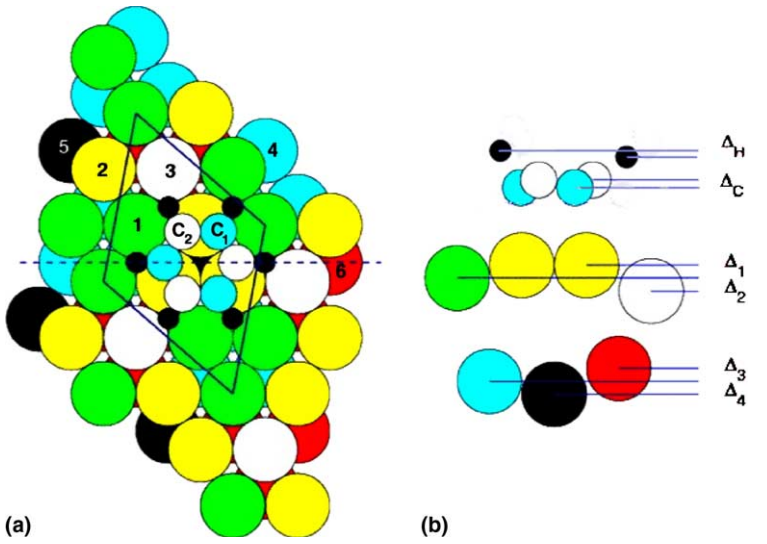

Fig. 2. Top (a) and side (b) views of the favored geometry calculated by LEED. Dashed line indicates the $[1\bar{1}00]$ direction. $p(\sqrt{7} \times \sqrt{7})$ unit cell is shown with a solid line. The inequivalent Co atoms in the first two layers and the C atoms are indicated by different numbers.

was found to be 2.26 ± 0.09 Å, which is 10% expanded compared to 2.04 Å, which is the sum of the metallic radius of cobalt and the covalent radius of carbon in single bond. The carbon ring remains nearly unchanged with respect to the gas phase, with negligible buckling of 0.01 ± 0.11 Å (Δ_C) between the two inequivalent carbon atoms (C_1/C_2). Carbon–hydrogen bonds are slightly expanded compared to the C–H bond in the gas phase benzene (1.08 Å) being 1.1 ± 0.2 Å. Buckling between the hydrogen atoms (Δ_H) is within the errorbars of the analysis (0.04 ± 0.4 Å). The vertical distance between the center of mass of the carbon ring and the center of mass of the H atoms is 0.3 ± 0.2 Å (dz_{H-C}), with the hydrogen atoms lying higher than the center of mass of the carbon ring.

Benzene adsorption induces some changes to the substrate structure. The first interlayer spacing (dz_{12}) remains similar to the bulk value (2.03 ± 0.10 Å). The second (dz_{23}) interlayer spacing is expanded by 3% (2.09 ± 0.10 Å) and the third (dz_{34}) interlayer spacing is contracted by 3% (1.97 ± 0.10 Å). The interlayer spacings are quoted between the centers of mass of the layers. Because of the strong buckling in the first layer, interlayer spacings quoted between the centers of mass do not give a realistic picture about the situation between the first two cobalt layers. Cobalt atoms right below the benzene ring (atom 2 in Fig. 2(a)) are pulled up by 0.10 ± 0.06 Å compared to the center of mass of the other atoms in the first layer (atoms 1 and 3 in Fig. 2(a)), which are almost planar. The interlayer spacing between the center of mass of the second layer and the center of mass of the atoms 1 and 3 (Fig. 2(a)) in the first layer is contracted by 2% compared to the bulk interlayer spacing. Average bucklings within the first three Co layers with respect to the center of mass of the layer are 0.05 ± 0.07 Å, 0.01 ± 0.13 Å and 0.03 ± 0.08 Å respectively. The height differences between the inequivalent Co atoms in the first two layers (Δ_1, Δ_2, Δ_3 and Δ_4) are 0.09 ± 0.06 Å, 0.01 ± 0.09 Å, 0.01 ± 0.07 Å and 0.0 ± 0.3 Å respectively (see Fig. 2(b)).

Table 2 shows the main geometric parameters which can be identified with the help of Fig. 2. Fig. 3 shows the theory–experiment agreement. In Fig. 3 it can be seen that the theory–experiment agreement is excellent for the integral order beams. In all the beams the relative intensities agree very well although it should be noted that the Pendry *R*-factor is only sensitive to the peak positions and not to the relative intensities. Fig. 3 also shows a schematic picture of the diffraction pattern where the indexes of the beams used in this analysis are shown. Two different domains that are related to each other by a mirror plane along $[1\,1\,\bar{2}\,0]$ direction are shown with different signs (○, □). The maximum number of free geometrical parameters used in the search is 16, which gives an energy range of 92 eV per parameter. Held et al. [21] have noted in the case of benzene adsorption on Ni{1 1 1} that large number of geometrical parameters for more asymmetrical structures reached the minimum energy range appropriate per geometrical parameter which they said to be 62 eV. For

Table 2
The main geometric parameters with the associated error bars from the LEED and DFT–GGA calculations

Overlayer			Substrate		
Parameter	Value (Å)		Parameter	Value (Å)	
	LEED	DFT–GGA		LEED	DFT–GGA
C–Co	2.26 ± 0.09	2.104	Δ_1	0.09 ± 0.06	0.191
dz_{C-Co}	2.20 ± 0.09	1.964	Δ_2	0.01 ± 0.09	0.036
C–C	1.39 ± 0.11	1.446	Δ_3	0.01 ± 0.07	−0.017
H–C	1.1 ± 0.2	1.091	Δ_4	0.0 ± 0.3	−0.082
dz_{H-C}	0.3 ± 0.2	0.392	dz_{12}	2.03 ± 0.10	1.980
Δ_C	0.01 ± 0.11	0.0	dz_{23}	2.09 ± 0.10	2.024
Δ_H	0.04 ± 0.4	0.0	dz_{34}	1.97 ± 0.10	1.999

Different parameters can be identified with the help of Fig. 2. In the DFT–GGA results negative sign indicates that the relaxation occurs in opposite direction with respect to the relaxation produced by the LEED calculation.

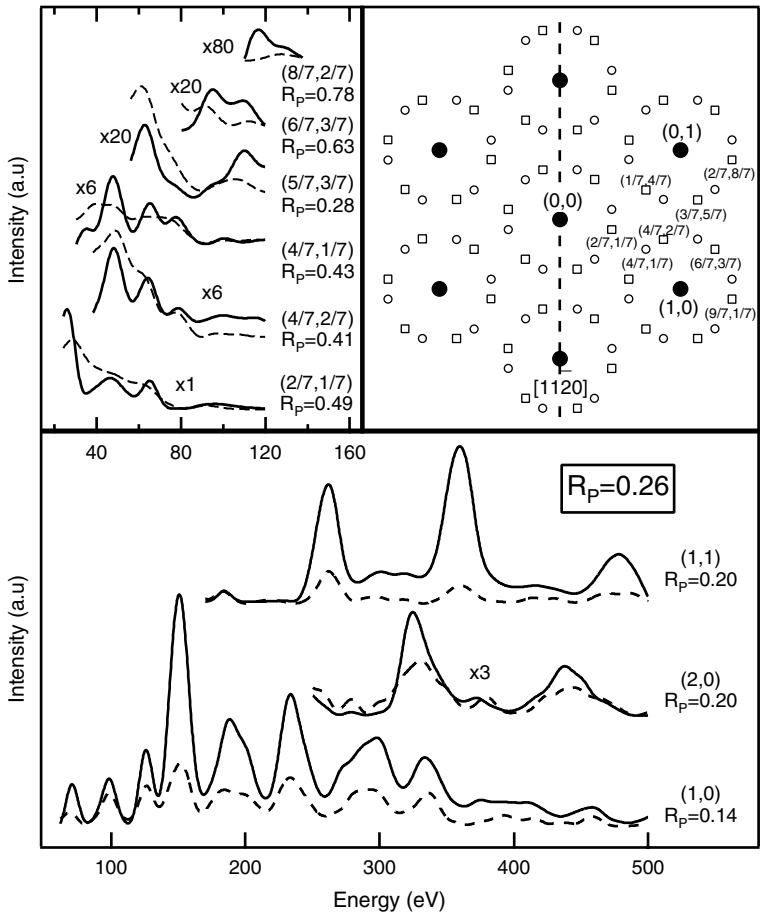

Fig. 3. Theory–experiment agreement. Dashed line corresponds to theory and solid line to experiment. Right upper corner shows a schematic figure of the diffraction pattern with the beam indexes showing the beams that are used in this calculation. The two different domains that are related by a mirror plane along $[1\,1\bar{2}\,0]$ are marked with different signs (○, □).

comparison our energy range per geometrical parameter is about 120% of that in the study of Pussi et al. (∼75 eV) [12] and 75% of that in the study of Held et al. (∼120 eV) [21].

In the density functional calculations the adsorption at the hcp A and B, fcc A and B, top A and B, and bridge A sites was investigated. The bridge B site was not studied, because the adsorption energy of bridge A was about 0.25 eV higher than at the hcp A and fcc A, which represent the energetically the lowest and practically degenerate adsorption sites. However, since the LEED experiment unambiguously prefers the hcp A site, it was concentrated on. In the following results only for this adsorption site are presented. The hcp B configuration is about 50 meV less favorable, the fcc B 0.14 eV and the top sites about 1.05 eV than at the minimum sites.

The optimized geometry from the density functional calculations is shown in Table 2. The carbon atoms of the benzene molecule lie 1.96 Å above the first surface layer and the carbon ring is slightly expanded. Large buckling was found for the first cobalt layer (0.19 Å). This buckling is noticeably larger than the buckling found in the LEED analysis. The buckling in the first substrate layer has been qualitatively different in the various DFT calculations published so far: at Ru{0001} [21] the

Table 3
The main vibrational frequencies from DFT–GGA calculations

Mode		C_6H_6(g)	C_6D_6(g)	C_6H_6(a)	C_6D_6(a)	C_6H_6/Rh{1 1 1}
ν_1	CH stretch	3132	2321	3090	2281	3113
ν_2	Ring stretch	994	948	865	829	870
ν_4	Out of plane bend	670	491	760	548	762
ν_9	CH bend	1341	1337	1313	1307	1339
ν_{10}	Ring stretch	1144	814	1129	800	1141
ν_{C-M}		–	–	328	326	366
		–	–	324		362
		–	–			344

The modes either belong to the A_1 representation of the C_{3v} symmetry group (ν_1, ν_2, ν_4, ν_9, ν_{10}), or are the modes of the benzene molecule against the surface (ν_{C-M}). The results for C_6H_6/Rh{1 1 1} are from Ref. [25].

buckling is in the range of 0.03 Å and at Ni{1 1 1} and Pt{1 1 1} around 0.15–0.20 Å [22–24], whereas in the experiments it has always been small. The origin of this difference is difficult to guess; the molecular dynamics simulations have been performed employing the present DFT–GGA technique to exclude the possible explanation that the calculations have been optimized at zero temperature: The buckling is practically unchanged in our *first-principles* molecular dynamics run compared with the zero-temperature geometry. The other parameters agree well with the experimental values, the deviations being of the order (ca. within 0.05 Å or better) generally seen in similar adsorption systems. From our calculations we find a work function of 5.05 eV for the clean Co{0 0 0 1} surface and 3.38 eV for the surface covered with the benzene.

Table 3 lists those (harmonic) vibrational frequencies from the density functional calculations which belong to the A_1 representation of the C_{3v} symmetry group. The whole symmetry group of the system is C_3, but the deviation of the geometry of the benzene ring is so small (less than 10^{-3} Å) that locally it can be seen having the higher symmetry. This excludes some of the modes, which however would have a very small intensity. Also shown are the frequencies of benzene on Rh{1 1 1} from Ref. [25].

During the LEED analysis also another minimum structure was discovered. This geometry was almost the same for the substrate cobalt (all parameters within the errorbars of the parameters reported here) but for the position of hydrogen atoms a difference was found. In this alternative structure the H atoms were located below the C-ring of the benzene molecule. The theory–experiment agreement for this structure was slightly better than for the structure reported in this paper ($R_P = 0.24$). However in the light of the DFT analysis performed, this structure is considered to be less favorable.

5. Discussion

In the study of C_6H_6 on Co{1 0 $\bar{1}$ 0} by Pussi et al. [12] the geometry consists of a molecular ring where the carbon atoms are buckled into a 'boat-like' geometry. The carbon–carbon bond lengths are expanded with respect to the gas-phase value to 1.50 ± 0.20Å, 1.53 ± 0.14 Å and 1.60 ± 0.30 Å. This is suggestive of significant weakening of the carbon–carbon bonds. The strong buckling and stretching of the C–C bonds is not inkeeping with this analysis. Thus this might be suggestive of the fact that the strong deformation of the benzene molecule is a consequence of the open {1 0 $\bar{1}$ 0} surface. On the Co{1 0 $\bar{1}$ 0} surface, values between 2.02 Å and 2.43 Å were found for the carbon–cobalt bonds [12]. The value of 2.26 ± 0.09 Å found in this analysis falls into the middle of this range.

A good comparison to this study is found in the paper of Braun et al. where the adsorption of benzene on Ru{0 0 0 1} (Ru is 5% bigger atom than Co) has been studied by LEED [10]. They found the favored adsorption site to be a hcp B site, compared to our hcp A site. The shortest C–Ru dis-

tance was 2.11 Å, which is similar to the sum of ruthenium covalent radii (1.32 Å) and the carbon single bond radius (0.78 Å) of 2.10 Å. The average distance between the benzene ring and the first ruthenium layer was found to be 2.09 Å. Buckling in the benzene ring was 0.08 Å which is slightly larger than in our study. Interlayer spacings in ruthenium changed upon benzene adsorption so that the first one was contracted (4%) and the second one was expanded (1%). The numerical values found by Braun et al. [10] compare quite well with this study, although the carbon ring seems to bond more strongly to Ru than to Co.

In the photoelectron diffraction study of Schaff et al. the structure of Ni{1 1 1}-p($\sqrt{7} \times \sqrt{7}$) $R19.1°$–C_6H_6 was investigated [4]. They found that benzene was adsorbed on a hcp A site (similar site to ours but on fcc{1 1 1} surface) with small Kekulé type distortions which gave rise to two different carbon–carbon bond lengths (1.40/1.44 ± 0.10 Å) within the carbon ring. The magnitude of these distortions was however within the error bars of the analysis. These carbon–carbon bond lengths are thus similar to what was found in our study. The perpendicular distance between benzene and the first Ni layer was 1.91 ± 0.04 Å and buckling in the first Ni layer was 0.10 ± 0.11 Å.

Density functional calculations have previously been performed for benzene on other close-packed transition metal surfaces like Ru{0 0 0 1} [26], Ni{1 1 1}, Ni{1 0 0} and Ni{1 1 0} [22,23], Rh{1 1 1}, Pd{1 1 1} and Pt{1 1 1} [25,27], Cu{1 1 0} [28], Cu{0 0 1} [29] and Al{1 1 1} [30]. In all these studies the carbon ring, or the C–C bond length, expands from the gas phase value about 0.05 Å and the hydrogen atoms are about 0.35 Å higher than the carbon atoms, in agreement with our DFT results on Co{0 0 0 1}. Also the small alternation in the C–C bond lengths, in our case 1.434/1.457 Å, is reproduced. We find an average height of the carbon ring above the first layer to be 1.96 Å, again close to the consensus of other DFT investigations.

The preferred adsorption site of benzene on Co{0 0 0 1} is not unambiguous in our DFT–GGA calculations, as hcp A and fcc A sites yield practically identical adsorption energy. Thus the reliable assignment comes only from the experiments, which in this case support the hcp A site, the other one of the DFT–GGA minima. In the earlier studies on the fcc{1 1 1} surfaces of Ni, Rh and Pd [22,25] the assignment is as well problematic, leading either to discrepancies with part of the experimental data or suggestions that the adsorbed structure might consist of domains with different adsorption sites. Thus we conclude that either the adsorption of benzene is rather subtle, or the DFT–GGA functionals have a difficulty assigning the correct adsorption site unambiguously, similarly to CO adsorbed on Pt{1 1 1} [31].

The DFT–GGA vibrational frequencies in Table 3, however, differ from the values of Morin et al. [25] on Rh{1 1 1}, Pd{1 1 1} and Pt{1 1 1}, being lower at all the five A_1 frequencies. It would be interesting to perform the calculation on all these surfaces with identical parameters, until then there remains some doubt whether this change is due to the details of the calculation, or it is physical due to the different electronic structure of the substrate. In any case, the metal–carbon distance is 0.1 Å smaller on Co{0 0 0 1} than on the other three surfaces, possibly leading to a stronger occupation of the π-orbitals of benzene upon adsorption, leading to a weakening of the C–C force constants and lowering of vibrational frequencies.

The experimental work function of the clean and benzene-covered Co{0 0 0 1} surface have been measured to be 5.55 and 4.25 eV in Ref. [32] and present work, respectively. The corresponding DFT values are 5.05 and 3.38 eV, yielding a reduction of the work function by 1.67 eV compared to the experimental drop of 1.3 eV. The underestimation of the absolute work functions is typical for the DFT–GGA calculations. On Ni{1 1 1} the change in work function is in DFT–GGA −1.83 eV at the hollow and −1.77 eV at the bridge site [22], experimentally −1.5 eV [6]. Thus the qualitative agreement between Co{0 0 0 1} and Ni{1 1 1} is good, even when the experimental and DFT–GGA do not agree quantitatively.

6. Conclusions

In this study the adsorption of benzene on Co{0 0 0 1} surface has been investigated by

Tensor-LEED and DFT calculations. The benzene molecule is found to adsorb on a hcp site with the two parallel C–C bonds aligned in $[1\bar{1}00]$ direction. The carbon–carbon bonds remain at their gas phase value and only small buckling is observed in the carbon ring. Compared to other studies of benzene adsorption on close packed surfaces, our results indicate that the molecule is more loosely bounded to the Co{0001} surface than to the other close packed surfaces in earlier studies.

Acknowledgment

This work was supported by the Materials Physics graduate school of Finland and Academy of Finland.

References

[1] K.M.E. Habermehl-Ćwirzeń, J. Katainen, J. Lahtinen, P. Hautojärvi, Surf. Sci. 507–510 (2002) 57.
[2] H.-P. Steinrück, J. Phys.: Condens. Matter 8 (1996) 6465.
[3] A.M. Bradshaw, D.P. Woodruff, in: Applications of Synchrotron Radiation High Resolution Studies of Molecules and Molecular Adsorbates on Surfaces, Springer, Berlin, 1995, p. 127.
[4] O. Schaff, V. Fernandez, Ph. Hofmann, K.-M. Schindler, A. Theobald, V. Fritzsche, A.M. Bradshaw, R. Davis, D.P. Woodruff, Surf. Sci. 348 (1996) 89.
[5] W. Huber, P. Zebisch, T. Bornemann, H.-P. Steinrück, Surf. Sci. 258 (1991) 16.
[6] W. Huber, H.-P. Steinrück, T. Pache, D. Menzel, Surf. Sci. 217 (1989) 103.
[7] C. Stellwag, G. Held, D. Menzel, Surf. Sci. 325 (1995) L379.
[8] P. Jacob, D. Menzel, Surf. Sci. 201 (1988) 503.
[9] A. Wander, G. Held, R.Q. Hwang, G.S. Blackman, M.L. Xu, P. de Andres, M.A. Van Hove, G.A. Somorjai, Surf. Sci. 249 (1991) 21.
[10] W. Braun, G. Held, H.-P. Steinrück, C. Stellwag, D. Menzel, Surf. Sci. 475 (2001) 18.
[11] C.J. Barnes, M. Valden, M. Pessa, Surf. Rev. Lett. 7 (2000) 67.
[12] K. Pussi, M. Lindroos, C.J. Barnes, Chem. Phys. Lett. 341 (2001) 7.
[13] H. Wadepohl, K. Büchner, M. Herrmann, H. Pritzkow, J. Organomet. Chem. 573 (1999) 22.
[14] M.A. Van Hove, W. Moritz, H. Over, P.J. Rous, A. Wander, A. Barbieri, N. Materer, U. Starke, G.A. Somorjai, Surf. Sci. Rep. 19 (1993) 191.
[15] A. Barbieri, M.A. Van Hove, private communication.
[16] A. Wander, M.A. Van Hove, G.A. Somorjai, Phys. Rev. Lett. 67 (1991) 626.
[17] J.B. Pendry, J. Phys. C: Solid State Phys. 13 (1980) 937.
[18] J.P. Perdew, J.A. Chevary, S.H. Vosko, K.A. Jackson, M.R. Pederson, D.J. Singh, C. Fiohais, Phys. Rev. B 46 (1992) 6671.
[19] Specifically, we used the Vienna ab initio simulation package— G. Kresse, J. Furthmüller, Phys. Rev. B 54 (1996) 11196; and described the electron-ion using the projector augmented wave method—P.E. Blöchl, Phys. Rev. B 50 (1994) 17953;
G. Kresse, D. Joubert, Phys. Rev. B 59 (1999) 1758.
[20] C. Kittel, Introduction to Solid State Physics, 6th ed., Wiley, New York, 1986.
[21] G. Held, M. Bessent, S. Titmuss, D.A. King, J. Chem. Phys. 105 (1996) 11305.
[22] F. Mittendorfer, J. Hafner, Surf. Sci. 472 (2001) 133.
[23] S. Yamagishi, S.J. Jenkins, D.A. King, J. Chem. Phys. 114 (2001) 5765.
[24] C. Morin, D. Simon, P. Sautet, J. Phys. Chem. B 107 (2003) 2995.
[25] C. Morin, D. Simon, P. Sautet, J. Phys. Chem. B 108 (2004) 5653.
[26] G. Held, W. Braun, H.-P. Steinrück, S. Yamagishi, S.J. Jenkins, D.A. King, Phys. Rev. Lett. 87 (2001) 216102.
[27] M. Sayes, M.-F. Reyniers, G.B. Marin, M. Neurock, J. Phys. Chem. B 106 (2002) 7489.
[28] B.L. Rogers, J.G. Shapter, M.J. Ford, Surf. Sci. 548 (2004) 29.
[29] N. Lorente, M.F.G. Hedouin, R.E. Palmer, M. Persson, Phys. Rev. B 68 (2003) 155401.
[30] R. Duschek, F. Mittendorfer, R.I.R. Blyth, F.P. Netzer, J. Hafner, M.G. Ramsey, Chem. Phys. Lett. 318 (2000) 43.
[31] P.J. Feibelman, B. Hammer, J.K. Nørskov, F. Wagner, M. Scheffler, R. Stumpf, R. Watwe, J. Dumesic, J. Phys. Chem. B 105 (2001) 4018.
[32] T. Vaara, J. Vaari, J. Lahtinen, Surf. Sci. 395 (1998) 88.